LBL-38404
UC-408
Preprint

Lawrence Berkeley Laboratory
UNIVERSITY OF CALIFORNIA

Submitted to ~~Journal of Applied Physiology~~ AMERICAN JOURNAL OF PHYSIOLOGY

Kinetic Analysis of Rubidium and Thallium as Deposited Myocardial Blood Flow Tracers in Isolated Rabbit Heart

R.C. Marshall, S.E. Taylor, P. Powers-Risius, B.W. Reutter, A. Kuruc, P.G. Coxson, R.H. Huesman, and T.F. Budinger

April 1996

Donner Laboratory

Biology & Medicine Division

Prepared for the U.S. Department of Energy under Contract Number DE-AC03-76SF00098

DISCLAIMER

LBL-38404
UC-408

Kinetic Analysis of Rubidium and Thallium as Deposited Myocardial Blood Flow Tracers in Isolated Rabbit Heart

Robert C. Marshall*‡, Scott E. Taylor*, Patricia Powers-Risius*, Bryan W. Reutter*, Alvin Kuruc*, Pamela G. Coxson*, Ronald H. Huesman*, and Thomas F. Budinger*

*Center for Functional Imaging
Life Science Division
E. O. Lawrence Berkeley National Laboratory
University of California
Berkeley, California 94720

‡Martinez Veterans Administration
Northern California System of Outpatient Clinics
Martinez, California 94553

April 1996

This work was supported in part by the Director, Office of Energy Research, Office of Health and Environmental Research, Medical Applications and Biophysical Research Division of the U.S. Department of Energy under Contract No. DE-AC0376SF00098 and National Institute of Health Grant Nos. HL25840 and HL48068.

Kinetic Analysis of Rubidium and Thallium as Deposited Myocardial Blood Flow Tracers in Isolated Rabbit Heart

Robert C. Marshall*‡, Scott E. Taylor*, Patricia Powers-Risius*, Bryan W. Reutter*, Alvin Kuruc*, Pamela G. Coxson*, Ronald H. Huesman*, and Thomas F. Budinger*

*Center for Functional Imaging
Life Science Division
E. O. Lawrence Berkeley National Laboratory
University of California
Berkeley, California 94720

‡Martinez Veterans Administration
Northern California System of Outpatient Clinics
Martinez, California 94553

Abstract

Evaluation of myocardial perfusion with deposited flow tracers such as thallium and rubidium is based on the assumption that tissue tracer content is proportional to flow. The purpose of this study was to evaluate the relationship between flow and tissue tracer content of thallium-201 and rubidium-83 in the isolated perfused rabbit heart. The multiple indicator dilution technique was employed with two independent computational approaches. The first approach explicitly deconvolved thallium-201 and rubidium-83 venous concentration curves by the intravascular reference tracer curve. The second approach used a conventional analysis. Both approaches showed that there was considerably more early washout of extracted rubidium-83 than thallium-201 and that the net retention of thallium-201 was greater than rubidium-83 as early as 2 min after isotope introduction. Since clinical assessment of myocardial perfusion with rubidium uses the short-lived (76 s) positron-emitting isotope rubidium-82, the rapid washout of rubidium-83 (86 d half-life) might not adversely affect the use of rubidium-82.

Introduction

Scintigraphic evaluation of myocardial perfusion with deposited flow tracers such as thallium-201 (^{201}Tl) and rubidium-82 (^{82}Rb) is based on the assumption that myocardial tracer content is

directly proportional to blood flow. Tissue tracer content would be proportional to flow if there were complete extraction and retention of the tracer traversing the heart. However, current evidence suggests that small, charged solutes in plasma, such as rubidium and thallium, are not completely extracted, or, once extracted, completely retained by the heart (2, 8, 9, 12, 13, 17, 18, 21, 23). There are, therefore, potential inaccuracies when using tissue ^{201}Tl and ^{82}Rb content to evaluate myocardial perfusion.

Substantial intravascular dispersion and recirculation of tracer are inevitable in *in vivo* studies. To avoid this, many investigators have evaluated thallium and rubidium extraction, retention, and washout in isolated skeletal muscle or myocardial preparations using a number of different species (8, 12, 13, 18, 21, 24). Although many reports focused on initial tracer extraction, several investigators also evaluated washout of extracted rubidium (11) or thallium (8, 9, 21). However, to the best of our knowledge, there are no data currently available simultaneously evaluating and comparing the extraction, retention, and washout of these two flow tracers in an isolated cardiac preparation.

The purpose of the present study was to investigate and compare the relationship between flow and tissue tracer content of thallium and rubidium by simultaneously measuring their extraction, retention, and washout in the myocardium at plasma flow rates ranging from 0.5 to 2.72 ml $min^{-1}gm^{-1}$ wet weight. We used the isolated, isovolumic retrograde red blood cell plus albumin (RBC/albumin) perfused rabbit heart to assess myocardial flow tracer kinetics following introduction of isotope as a compact bolus in the absence of recirculation. The multiple indicator dilution technique (5) was used to simultaneously acquire information on rubidium and thallium in the presence of an intravascular reference tracer, iodine-125-albumin (^{125}I-albumin). Data obtained using this technique were analyzed in two distinct ways. The first approach, previously used by Kuruc et al. (14) for the kidney, explicitly deconvolved the thallium and rubidium venous concentration curves by the albumin curve to separate the effects of circulatory dispersion from myocardial extraction and retention of thallium and rubidium. In the second approach, the venous concentration curves were used to compute ^{201}Tl and ^{83}Rb extraction, retention, and washout using a conventional analysis as previously described by Crone (6), Lassen and Crone (15), Bassingthwaighthe et al. (2), Guller et al. (10), and Little et al. (19).

Methods

Experiment Preparation

Preparation of isovolumic, retrograde RBC/albumin perfused rabbit hearts was similar to that reported previously (21, 22). All procedures were done in accordance with institutional guidelines for animal research. Non-fasted, male New Zealand White rabbits were given 4000 units sodium

heparin (Upjohn Co., Kalamazoo, MI) and 250 mg sodium pentobarbital (Abbott Labs, North Chicago, IL) via an ear vein. The heart was immediately excised through a median sternotomy and arrested in ice-cold buffer. The aorta was then rapidly attached to a cannula to allow retrograde perfusion with RBC/albumin buffer perfusate. An apical drain was inserted via the left atrium through the left ventricular apex to drain fluid from the Thebesian circulation and any leakage through the aortic valve. After the atrio-ventricular node was crushed to allow controlled stimulation, a fluid-filled latex balloon connected to a Gould-Statham P23ID pressure transducer (Gould, Inc., Oxnard, CA) was inserted into the left ventricle (LV) via the left atrium and mitral valve. The balloon was inflated to maintain end-diastolic pressure at 8–10 mmHg. Perfusion pressure and developed pressure were continuously recorded on a Graphtec Linearecorder (Western Graftec, Irvine, CA). A coronary venous sampling catheter and needle thermistor (Bailey Instrument Co., Inc., Saddlebrook, NJ) were inserted into the right ventricle via the right atrium and tricuspid valve. The venae cavae and pulmonary artery were ligated so all coronary venous drainage flowed out the sampling catheter. Stimulating electrodes connected to a Grass SD44 stimulator were placed against the left and right ventricles and 4 V, 4 ms stimuli were delivered at a rate of 180 min^{-1}. Temperature was maintained between 36°C and 38°C with a water-jacketed heating coil and heart chamber. Coronary flow was held constant with a peristaltic pump (Ranin Instrument Co., Woburn, MA) and the RBC/albumin perfusate was not recirculated. The rate of coronary blood flow was measured as the blood exited from the coronary venous sampling catheter. Control flow rate was approximately 1.5 ml min^{-1} g^{-1} wet wt LV. The perfusion line included an in-line 20 micron blood transfusion filter (Statcorp, Inc., Columbia, TN) to remove red blood cell aggregates.

Hearts were perfused with a modified Tyrode's solution containing oxygenated bovine erythrocytes and 17 g/l bovine serum albumin (Fraction V, fatty-acid free, Sigma Chemical Co., St. Louis, MO). The bovine serum albumin was dialyzed overnight at 4°C against buffer and filtered through a 0.8 micron Millipore filter. Fresh bovine red cells were used the same week they were obtained. The cells were separated from whole blood by centrifugation in 250 ml polyethylene bottles at 2800 *g* for 20 min at 6°C, then washed, resuspended with oxygenated ice-cold buffer, and spun again; this separation procedure was repeated four times. The specific electrolyte concentrations of the buffer solution (pH 7.3–7.4) were: 110 mM NaCl, 2.5 mM $CaCl_2$, 6 mM KCl, 1 mM $MgCl_2$, 0.435 mM NaH_2PO_4, and 28 mM $NaHCO_3$. Glucose (5.6 mM) and sodium pyruvate (2 mM) were added to ensure adequate substrate availability. Measurements of pH and the levels of carbon dioxide and oxygen were done on the RBC/albumin perfusate and on selected venous samples using an IRMA™ Blood Gas Analyzer (Diametrics Medical, Inc., St. Paul, MN). Values were automatically calculated for bicarbonate, total carbon dioxide, base excess, and percent oxygen saturation. The concentration of red blood cells in the perfusate buffer was adjusted to a

hematocrit of 17–25%. The flask containing the RBC/albumin perfusate was gassed with a mixture of 98% O_2 + 2% CO_2 during the experiment.

Radiopharmaceuticals

The radioisotopes were purchased from the following sources: ^{125}I-albumin (bovine serum), E.I. DuPont deNemours & Co., Boston, MA; ^{201}Tl (thallous chloride), Mallinkrodt Medical, San Francisco, CA; ^{83}Rb (rubidium chloride), Los Alamos National Laboratory, Los Alamos, NM.

Experimental Protocol

After the heart was prepared, an equilibration period of at least 15 min preceded all experimental interventions. A heart was acceptable for study if it developed at least 80 mmHg pressure (peak-systolic minus end-diastolic) and if end-diastolic and end-systolic pressures were stable over the equilibration period. After equilibration, myocardial perfusion was gradually changed to the experimental flow rate and subsequently held constant by the perfusion pump. Each heart was evaluated at one flow rate. The range of flow rates evaluated, 0.51 to 2.72 ml min^{-1} g^{-1} wet wt LV, is associated with normal high energy phosphate content over the time periods studied here (20). Five to ten min after equilibration at the experimental flow rate, a mixed isotope bolus consisting of ^{125}I-albumin, ^{201}Tl, and ^{83}Rb (0.4–0.6 microcurie of each isotope in 0.2 ml RBC/albumin perfusate) was injected just above the aortic cannula. Rapid venous sampling (2–5 s per sample depending upon the flow rate) from the right ventricular cannula into pre-weighed vials commenced with radioisotope introduction and continued uninterrupted for 2 min. Subsequent samples were taken at progressively longer intervals (from 15–120 s) over a period of 20–30 min post-injection for a total of 75–90 samples. About 0.5 ml was collected for each sample. The sample vials were weighed again after collection to obtain the net weight.

Data Acquisition and Preliminary Data Processing

Venous samples and aliquots (n = 10) of a dilution of the mixed isotope injection solution were counted on a gamma counter (TM Analytic, Inc., Brandon, FL) enhanced with a MICRAD automated measurement system (MICRAD, Inc., Knoxville, TN). The computer-based Multi-Channel-Analyzer simultaneously quantified and recorded the spectrum from all isotopes in the sample. The results were stored on a computer and retrieved for analysis on a UNIX workstation. Reference standards for ^{201}Tl, ^{83}Rb, and ^{125}I-albumin were also counted. Each sample spectrum was decomposed into a linear combination of the spectra of the reference standards using a weighted least squares fit.

Myocardial extraction, retention, and washout of ^{201}Tl and ^{83}Rb were assessed from the directly measured venous activity. The venous activity was expressed as the fraction of injected

activity appearing per second, $h(t)$, that is, as a fractional venous appearance rate. The fractional venous appearance rate was computed by the formula

$$h(t) = \frac{FC_i(t)}{Q_o} \cdot \frac{1.026\ g}{ml} \qquad (1)$$

where F denotes the plasma flow in ml/s, $C_i(t)$ denotes the venous sample activity in counts s^{-1} g^{-1}, Q_0 denotes the injected activity in counts s^{-1}, and 1.026 g/ml is the density of plasma. The fractional venous appearance rates for an experiment with a plasma flow rate of 2.13 ml min^{-1} g^{-1} wet wt LV (experiment 950125 in Table I) are graphed in Fig. 1.

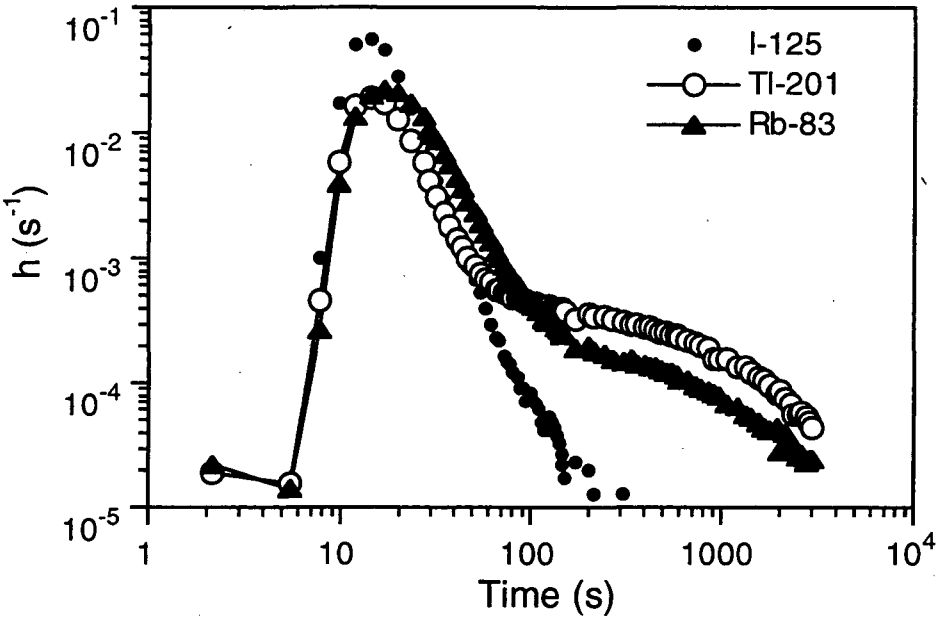

Figure 1. Fractional venous appearance rate, $h(t)$, of ^{201}Tl, ^{83}Rb, and ^{125}I-albumin.

Data Analysis

Myocardial Extraction, Retention, and Washout of ^{201}Tl and ^{83}Rb Using Deconvolution Analysis. The venous outflow curves for ^{201}Tl and ^{83}Rb are a function of circulatory dispersion, which is reflected in the venous outflow curve for albumin, as well as the extraction and retention of the tracer by the myocardium. This concept is schematically diagrammed in Fig. 2. In order to characterize the handling of the tracers by the myocardium in the simplest way, it is desirable to correct the diffusible tracer curves for the circulatory dispersion of the tracer as measured by the albumin curve. This was done by modeling the diffusible tracer curve as the response of a linear time-invariant system to an input consisting of the albumin curve. One can then estimate the response of the system as if the albumin curve were replaced with a narrow pulse. This response,

termed the impulse response of the system, provides a description of the myocardial extraction and retention of the tracer that is independent of circulatory dispersion (Fig. 3).

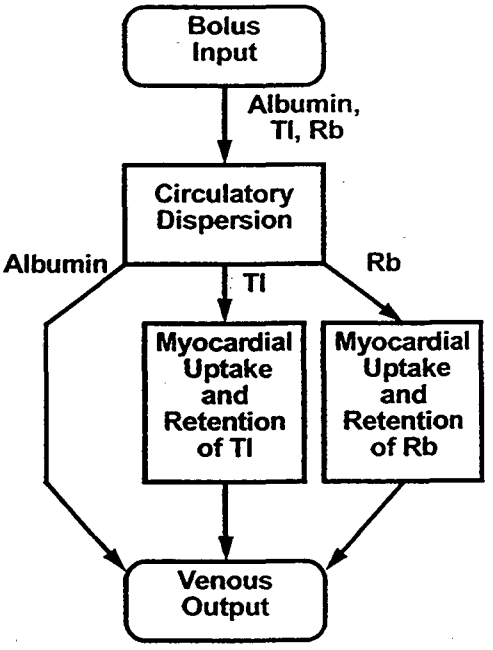

Figure 2. Schematic diagram showing the factors affecting the venous outflow curves of thallium, rubidium, and albumin. In interpreting Fig. 2, it should be recognized that the processes of circulatory dispersion and tracer extraction and retention overlap in time and space; the reader should not infer from the diagram that they are sequential.

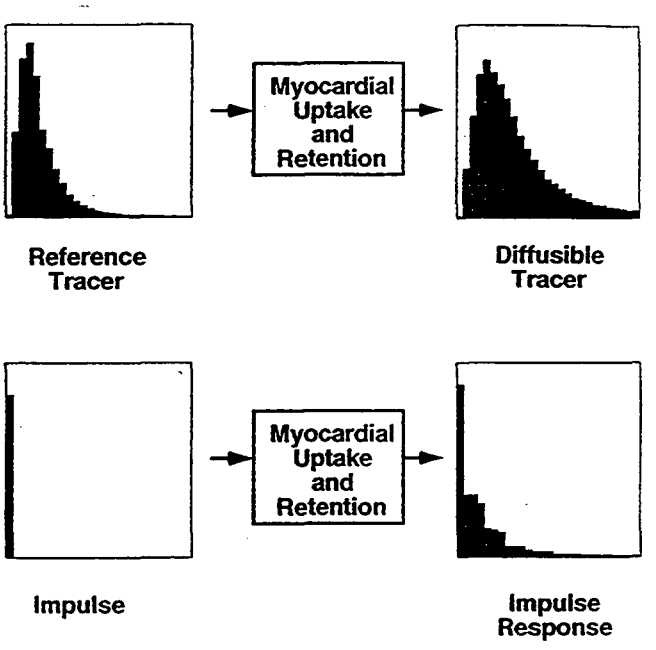

Figure 3. Viewing the curves from the reference and diffusible tracers as the input and output of a linear time-invariant system, we can compute the response of the system to an impulse input. The process of estimating the impulse response of the system from an input-output pair is termed deconvolution.

Let $h_R(t)$ and $h_D(t)$ denote the venous outflow curves for ^{125}I-albumin and ^{201}Tl or ^{83}Rb, respectively (R and D are intended as mnemonics for reference and diffusible tracer, respectively). We model $h_D(t)$ as the mathematical convolution of $h_R(t)$ and the impulse response of the system, $i(t)$:

$$h_D(t) = h_R * i(t)$$
$$\equiv \int_0^t h_R(\tau) i(t-\tau) d\tau \qquad (2)$$

where $*$ denotes the mathematical operation of convolution. The units of $i(t)$ are inverse time. Note that $i(t-\tau)$ is just a delayed, by τ, copy of $i(t)$. Thus this equation expresses $h_D(t)$ as the superposition of copies of $i(t)$ that are scaled and time-shifted according to the input function, $h_R(t)$. Physically, the impulse response may be thought of as quantifying the distribution of transit time

delays of the diffusible tracer relative to the reference tracer. That is, $\int_{t_0}^{t_1} i(t)dt$ is the fraction of the flow tracer whose transit time is delayed by times between t_0 and t_1, relative to the reference tracer. In these experiments, it is to be expected that a certain fraction, p, of the tracer will not be extracted at all, that is, will have the same kinetic behavior as the reference tracer. This would manifest itself in the impulse response as a sharp peak at time zero with area p.

Given $h_R(t)$ and $h_D(t)$, one can compute $i(t)$ by solving *Eq. 2*. This process is termed deconvolution. In practice, deconvolution is an ill-posed problem in the sense that small data errors can result in large errors in the computed impulse response (7). To circumvent this difficulty, we computed an approximate solution to *Eq. 1* that was non-negative and monotonically decreasing. It has been shown that these constraints are sufficient to give robust impulse response estimates (14).

Implementation of Deconvolution Analysis. Kinetic information on early and late tracer extraction, retention, and washout was obtained by: *1*) estimating the initial 180 s of the impulse response at a 5-s time resolution and; 2) estimating the impulse response over the duration of each experiment at a 60-s time resolution. First, venous tracer curves that were uniformly sampled in time were computed by numerical integration, assuming the venous concentration to be the (constant) measured value over each data collection interval. The impulse response estimate was obtained by minimizing the sum of the squared differences between the (resampled) diffusible tracer curve and the discrete convolution of the albumin and impulse response curves subject to the constraint that the impulse response is nonnegative and nonincreasing. The computed impulse response curve was obtained by solving for the nonnegative decrements of the impulse response and its final value using a numerically stable nonnegative least squares routine (16).

Myocardial Extraction, Retention, and Washout of ^{201}Tl and ^{83}Rb Using a Conventional Analysis. As initially proposed by Crone (6), we defined the instantaneous tracer extraction, $E(t)$ as

$$E(t) = \frac{h_R(t) - h_D(t)}{h_R(t)}. \qquad (3)$$

As in the deconvolution analysis, $h_R(t)$ is the fractional venous appearance rate of the reference tracer, ^{125}I-albumin, and $h_D(t)$ is the fractional venous appearance rate of the diffusible tracer, ^{201}Tl or ^{83}Rb. We defined peak instantaneous extraction, E_{peak}, to be the maximum value of $E(t)$, over the course of an experiment:

$$E_{peak} = \max E(t). \qquad (4)$$

Net tracer retention, $E_{net}(t)$ was defined by

$$E_{net}(t) = \frac{\int_0^t [h_R(\tau) - h_D(\tau)]d\tau}{\int_0^t h_R(\tau)d\tau} \quad (5)$$

where τ is a variable of integration.

Net tissue tracer uptake, *U(t)*, a function of tracer delivery as well as net retention, was defined to be the product of plasma flow and $E_{net}(t)$:

$$U(t) = F \times E_{net}(t). \quad (6)$$

Fractional escape rate, FER*(t)*, a measure of washout, was defined as the ratio of tracer fractional venous appearance rate, *h(t)*, and the tracer residue function:

$$\text{FER}(t) = \frac{h(t)}{R(t)} \quad (7)$$

where

$$R(t) = 1 - \int_0^t h(\tau)d\tau \ . \quad (8)$$

These computations, employed by Crone (6), Lassen and Crone (15), Bassingthwaighte et al. (2), Guller et al. (10), and Little et al. (19), have been previously used by us (21) and by other investigators (17, 18).

Volume of Distribution

One of the fundamental rationales for using the potassium analogs ^{201}Tl and ^{83}Rb as deposited flow tracers is that they are diluted in the large intracellular potassium pool once extracted by the myocyte. One method of assessing distribution within the intracellular potassium pool is to determine the volume of distribution (V_d) for these two tracers. V_d is the plasma volume equivalent required to dissolve ^{201}Tl and ^{83}Rb in tissue at the same concentration present in plasma. For the potassium analogs ^{201}Tl and ^{83}Rb, V_d would be expected to be greater than tissue volume because of the marked concentrative effect of sarcolemmal potassium transport. The volumes of distribution of ^{201}Tl and ^{83}Rb were examined in six experiments performed at different flow rates ranging from 0.3 to 2.1 ml min^{-1} g^{-1} wet wt LV. In each experiment, ^{201}Tl, ^{83}Rb, and ^{125}I-albumin were infused continuously for 120 min. After 90 min, there was no detectable arterial-venous difference for the two cationic tracers. V_d was estimated using the formula

$$V_d/V = CSG_{tissue} / CSG_{plasma} \quad (9)$$

where CSG_{tissue} is the counts s^{-1} g^{-1} wet wt LV, CSG_{plasma} is the average counts s^{-1} g^{-1} of the RBC/albumin perfusate, and V is the reciprocal of the specific gravity of the heart. The left

ventricle was weighed immediately after the experiment and counted on a gamma counter to obtain the counts s^{-1} g^{-1}. Tissue tracer activity was corrected for intravascular blood activity assuming that arterial and venous volumes are 11% of tissue volume (1).

Radioisotope Uptake Into Red Blood Cells

Although the bolus introduction technique used in this study does not provide much time for the isotope to penetrate red cells, there was usually a lag time of up to 15 min between addition of the isotopes to the RBC/albumin perfusate injection aliquot and the actual injection of 0.2 ml of this preparation into the arterial port. To investigate the uptake of ^{201}Tl and ^{83}Rb into the red blood cells during this lag time, aliquots of the injection mixture were taken at 0.5, 2, 5, 10, 15, 20, 25, and 40 min after the addition of isotope to the injection mixture. In a separate experiment, samples were taken from the right ventricle drain at 1, 5, 12, and 18 min after injection of the isotope mixture into the arterial port. In both experiments the red cell and plasma fractions were separated and counted as described in the experiment protocol and data analysis sections. There was 7.2% and 7.1% more uptake of ^{201}Tl than ^{83}Rb in the red blood cells at the 15 and 18 min time points, respectively. Both experiments suggest that ^{201}Tl is taken up preferentially in red blood cells. The percent isotope uptake from the first experiment is plotted in Fig. 4.

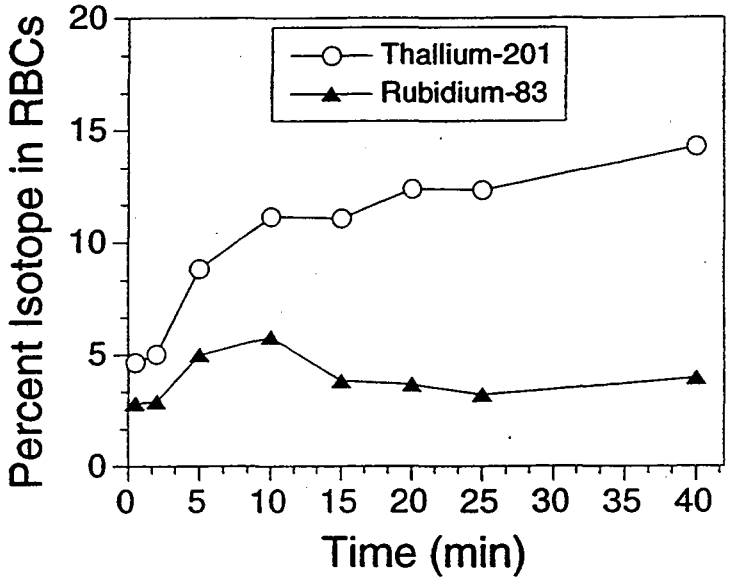

Figure 4. Uptake of ^{201}Tl and ^{83}Rb in bovine red blood cells as a function of time after their addition to the bolus injection preparation.

Statistics

Statistical values are given as mean ± SD. All statistical calculations were performed using StatView statistical software (Abacus Concepts, Inc., Berkeley, CA). Data used for regression analysis were fit to linear models with estimated regression coefficients derived by the unweighted least-squares method. Comparisons of kinetic parameters of ^{201}Tl and ^{83}Rb were performed with Student's two-tailed *t*-test for paired observations. A *P* value of less than 0.05 was considered statistically significant.

Results

We studied 21 isolated, isovolumic retrograde RBC/albumin perfused rabbit hearts at plasma flow rates of 0.51 to 2.72 ml min^{-1} g^{-1} wet wt LV. The results of an experiment with a plasma flow rate of 2.13 ml min^{-1} g^{-1} wet wt LV (experiment 950125 in Table I) are presented in Fig. 1, showing the indicator dilution curves, expressed as the fractional venous appearance rates, for ^{201}Tl, ^{83}Rb, and ^{125}I-albumin. The curves for ^{201}Tl and ^{83}Rb are similar in form to the ^{125}I-albumin curve except that the peak values are lower and the tail values are higher. During the initial portion of the curves, the smaller *h(t)* for ^{201}Tl and ^{83}Rb relative to ^{125}I-albumin reflect permeation of a fraction of these two cations from the intravascular space into the extravascular space. After about 20 s, the fractional venous appearance rate for ^{83}Rb exceeds that for ^{125}I-albumin due to back-diffusion of tracer from the extravascular space. After about 80 s, the fractional venous appearance for ^{201}Tl also exceeds that for ^{125}I-albumin, reflecting back-diffusion of this tracer from the tissue space into the intravascular space. During the last phase of the experiment, the fractional venous appearance rate for ^{201}Tl was approximately twice that of ^{83}Rb, while the fractional venous appearance rate of ^{125}I-albumin was negligible. These qualitative relationships were observed in all experiments reported here.

Tracer Extraction, Washout, and Retention using Deconvolution Analysis

Example of Computed Impulse Responses. Data from all 21 experiments were analyzed using the deconvolution analysis. As an example, the deconvolution results from the experiment shown in Fig. 1 are illustrated in Fig. 5. Fig. 5*A* shows the first 120 s of the computed impulse responses for ^{201}Tl and ^{83}Rb. The first time point on each of these curves reflects the fraction of tracer whose venous appearance curve is identical to that of the reference tracer, albumin, within the temporal resolution of the acquired data. This quantity is termed the pass-through fraction and is denoted by *p*. For this experiment, *p* was 33% and 29% for ^{201}Tl and ^{83}Rb, respectively. The fraction of tracer that is delayed relative to the reference tracer is $1 - p$. This quantity reflects movement of tracer from the intravascular to the extravascular space and is termed the extraction fraction. The

extraction fractions for this experiment were 67% and 71% for ^{201}Tl and ^{83}Rb, respectively. The subsequent time points of the impulse response curves reflect return of the extracted tracer. The principal difference between the curves for ^{83}Rb and ^{201}Tl is that the curve for ^{83}Rb decreases more rapidly than the curve for ^{201}Tl. Thus, while the extraction of ^{201}Tl is somewhat less than that of ^{83}Rb, there is much more rapid washout of extracted ^{83}Rb than ^{201}Tl. This washout can be quantified in terms of the total area under the impulse response between two given time points. For example, the washout of ^{201}Tl and ^{83}Rb between 5 and 30 s was 10% and 39% of the total tracer amounts, respectively. The consistency of the assumed linear, time-invariant system model with the data was assessed by comparing the convolution of the input function and the computed impulse response with the observed output curves. The relative root mean square error was 0.8% and 1.5% for ^{201}Tl and ^{83}Rb, respectively.

Fig. 5*B* shows the computed impulse responses for ^{201}Tl and ^{83}Rb over the duration of the experiment. The main feature of these curves is that, when plotted on a logarithmic scale, their tails are well approximated by a straight line. This indicates that their functional form is that of a single decaying exponential curve. The time constants of exponential fits to the tails of the ^{201}Tl and ^{83}Rb curves were 1310 and 1200 s, respectively. The areas under the fits corresponded to 66% and 24% of the total injected tracer, respectively. Again, the consistency of the assumed linear, time-invariant system model with the data was assessed by comparing the convolution of the input function and the computed impulse response with the observed output curves. The relative root mean square error was 0.003% and 0.034% for ^{201}Tl and ^{83}Rb, respectively.

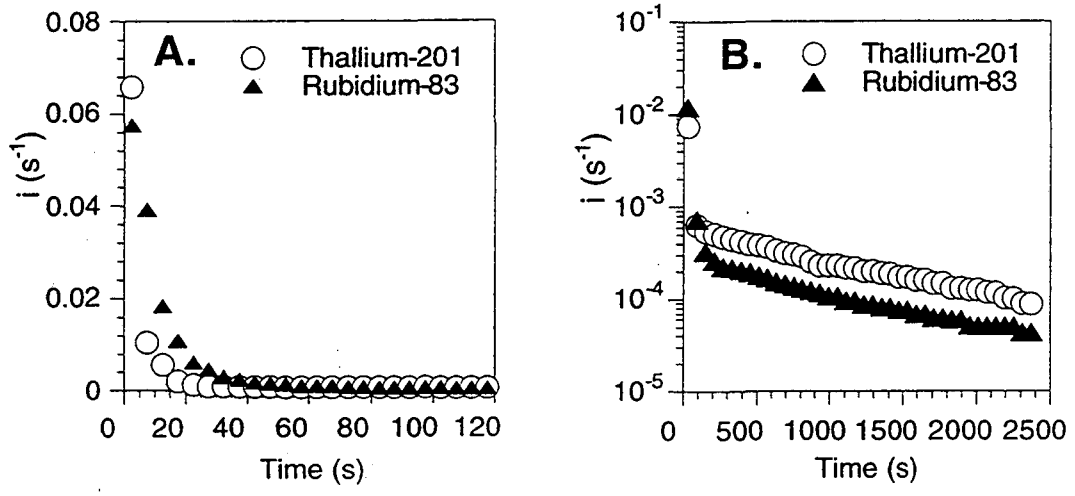

Figure 5. Deconvolution results from an experiment with a plasma flow rate of 2.13 ml min^{-1} g^{-1} wet wt LV. Computed impulse responses for ^{201}Tl and ^{83}Rb over the initial 120 s (panel *A*) and the duration of the experiment (panel *B*).

^{201}Tl and ^{83}Rb Extraction Fraction. Extraction fraction values for each experiment are listed in Table 1. The mean extraction fraction for ^{83}Rb (72 ± 10%) was significantly higher than that for ^{201}Tl (65 ± 9%) ($P < 0.0005$). The extraction fraction of ^{201}Tl tended to be negatively correlated with flow (with a slope of -0.038 ml^{-1} min g), but the correlation did not reach statistical significance ($P < 0.15$). The extraction fraction of ^{83}Rb had a statistically significant negative correlation with flow with a slope of -0.084 ml^{-1} min g ($P < 0.0025$).

^{201}Tl and ^{83}Rb Retention and Washout. Rapid washout of extracted tracer was assessed by computing the integral of the impulse response curves over the interval from 5 to 30 s. The mean integral for ^{201}Tl (6 ± 4%) was significantly smaller than that for ^{83}Rb (32 ± 6%) ($P < 0.0001$). Both tended to increase with flow (^{201}Tl, slope of 0.030 ml^{-1} min g, $P < 0.015$; ^{83}Rb, slope of 0.016 ml^{-1} min g, $P < 0.41$), but only ^{201}Tl had a statistically significant correlation with flow.

Myocardial retention of the flow tracers was estimated by examining the later portions of the impulse response curve. As illustrated in Fig. 5*B*, the tails of the impulse responses of both ^{201}Tl and ^{83}Rb were well described by decaying exponential functions. We therefore fit single decaying exponential curves to the tails of the impulse responses, starting at 40% of the total data acquisition time. The mean area under the exponential fits for ^{201}Tl (62 ± 13%) was more than twice as large than for ^{83}Rb (29 ± 10%) ($P < 0.0001$). Both areas were negatively correlated with flow with a slope of -0.11 ml^{-1} min g (^{201}Tl, $P < 0.0035$; ^{83}Rb, $P < 0.0001$).

The mean time constants of the exponential fits were 1270 ± 460 s and 1210 ± 340 s for ^{201}Tl and ^{83}Rb, respectively. The time constants were negatively correlated with flow with slopes of -400 s ml^{-1} min g ($P < 0.002$) and -280 s ml^{-1} min g ($P < 0.004$).

Myocardial Extraction, Retention, and Washout of ^{201}Tl and ^{83}Rb Using Conventional Analyses. As an example, the conventional analysis results from the experiment shown in Fig. 1 are plotted in Fig. 6. Instantaneous tracer extraction, $E(t)$, is plotted in Fig. 6*A*. $E(t)$ values for ^{83}Rb peak earlier and higher than those for ^{201}Tl. Net retention values, $E_{net}(t)$, (Fig. 6*B*) for ^{201}Tl and ^{83}Rb are highest about 10 s after tracer injection with maximum E_{net} occurring at the time of peak E. Subsequently, $E_{net}(t)$ values for the two flow tracers decline for the remainder of the experiment. Values for fractional escape rate, FER(t), (Fig 6*C*) for ^{83}Rb are higher than those for ^{201}Tl soon after the peak of the outflow dilution curves. This observation indicates that there is more early washout of ^{83}Rb than ^{201}Tl. FER(t) values for ^{201}Tl are greater than those for ^{83}Rb after about 100 s.

Table 1. Flow, hematocrit, and extraction parameters for each experiment

Exp. No.	Plasma Flow *ml min^{-1} g^{-1} wet wt LV*	Hct. %	Deconvolution Analysis *Extraction Fraction* ^{201}Tl	^{83}Rb	Conventional Analysis $E_{peak}(t)$ ^{201}Tl	^{83}Rb
940908	0.51	20.0	0.61	0.84	0.62	0.86
940615	0.52	17.0	0.83	0.77	0.85	0.82
940727	0.56	19.0	0.70	0.83	0.70	0.85
950201	0.58	18.0	0.71	0.75	0.75	0.84
940601	0.66	18.5	0.66	0.77	0.68	0.75
940719	0.83	17.0	0.71	0.88	0.72	0.86
940809	0.99	18.5	0.57	0.61	0.61	0.61
940708	1.08	18.0	0.57	0.72	0.66	0.79
940510	1.16	18.0	0.64	0.72	0.66	0.75
950207	1.25	18.0	0.71	0.74	0.74	0.82
940712	1.33	18.0	0.62	0.77	0.61	0.78
940802	1.36	18.0	0.77	0.83	0.77	0.88
940906	1.61	20.0	0.58	0.68	0.58	0.68
950208	1.73	25.0	0.60	0.69	0.61	0.74
940629	1.82	19.0	0.68	0.72	0.68	0.74
950214	2.04	20.0	0.44	0.46	0.57	0.51
950125	2.13	18.0	0.67	0.71	0.67	0.77
950215	2.31	19.5	0.72	0.75	0.73	0.77
950223	2.59	18.0	0.67	0.70	0.68	0.81
950321	2.72	18.5	0.55	0.56	0.60	0.66
940614	2.72	18.0	0.63	0.58	0.68	0.66
Mean		18.8	0.65	0.72	0.67	0.76
± SD		1.7	0.09	0.10	0.07	0.09

Table 1. Experiment Number (Exp. No.), plasma flow, percent hematocrit (Hct.), and extraction indices for ^{201}Tl and ^{83}Rb using deconvolution and conventional analyses. The extraction fraction obtained using the deconvolution analysis represents the fraction of flow tracer whose transit time was delayed relative to ^{125}I-albumin due to diffusion into the extravascular space. The values for $E_{peak}(t)$ using the conventional analysis are the highest instantaneous extraction values computed using *Eq. 3*.

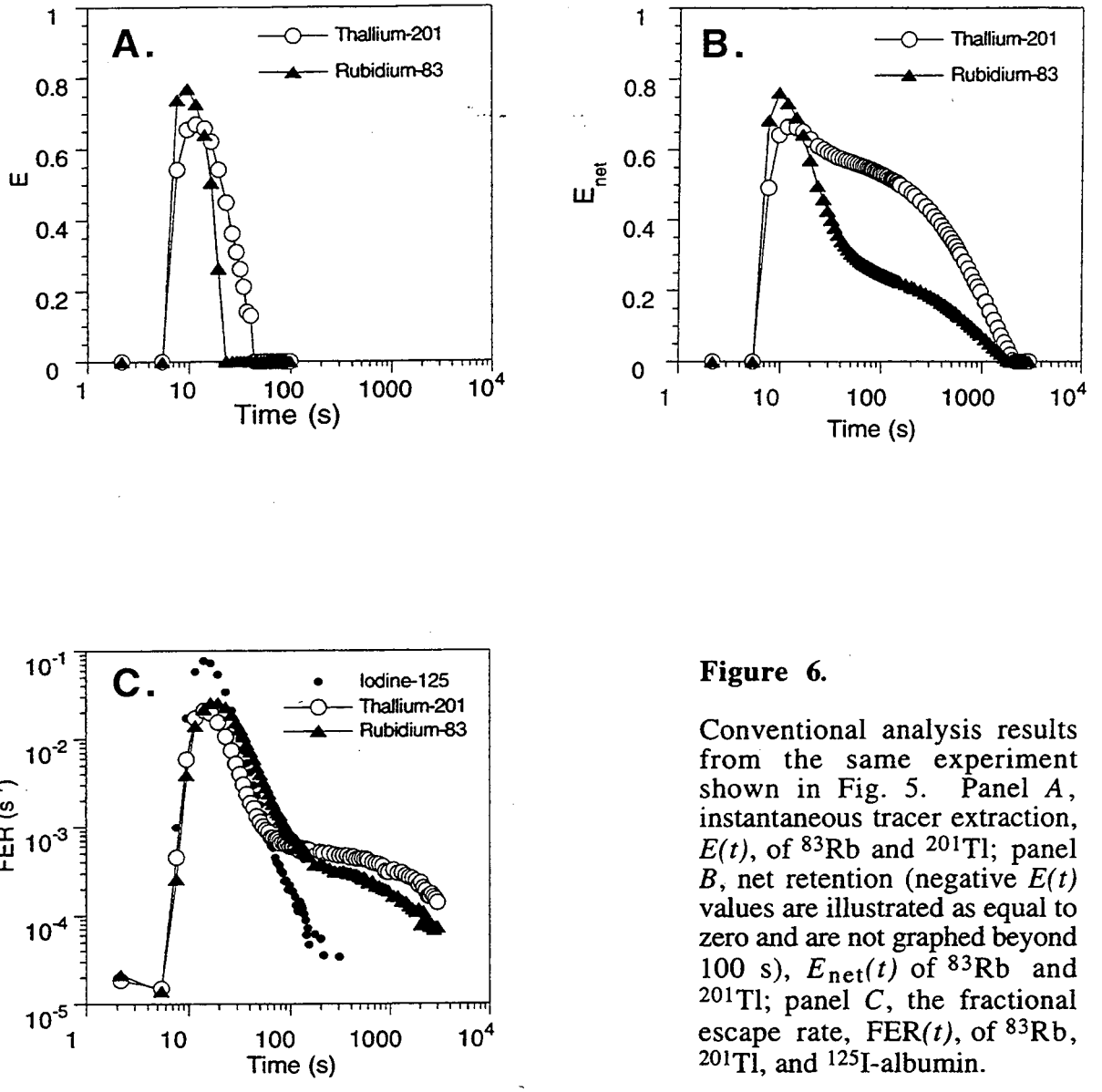

Figure 6.

Conventional analysis results from the same experiment shown in Fig. 5. Panel *A*, instantaneous tracer extraction, *E(t)*, of ^{83}Rb and ^{201}Tl; panel *B*, net retention (negative *E(t)* values are illustrated as equal to zero and are not graphed beyond 100 s), $E_{net}(t)$ of ^{83}Rb and ^{201}Tl; panel *C*, the fractional escape rate, FER*(t)*, of ^{83}Rb, ^{201}Tl, and ^{125}I-albumin.

^{201}Tl and ^{83}Rb Peak Instantaneous Extraction. Values for peak instantaneous extraction, E_{peak}, for ^{201}Tl and ^{83}Rb are given in Table I for each experiment. The mean E_{peak} for rubidium (0.76 ± 0.09) is similar to that previously reported for thallium (3, 21, 25) for the range of flows evaluated here. The mean E_{peak} for thallium (0.67 ± 0.07) was lower than that for rubidium, possibly reflecting red cell sequestration. These results are similar to those obtained using the deconvolution analysis. No significant correlation between flow and ^{201}Tl peak extraction was observed (slope of -0.034 ml^{-1} min gm, $P < 0.25$), while ^{83}Rb peak extraction and flow were negatively correlated (slope of -0.070 ml^{-1} min g, $P < 0.045$).

^{201}Tl and ^{83}Rb Fractional Escape Rate. In Fig. 6*C*, the fractional escape rate for ^{83}Rb is seen to exceed that for ^{201}Tl for approximately 1 min following the peak of the indicator dilution curve. To further evaluate early FER, we analyzed values at the point of the maximal percent difference between ^{201}Tl and ^{83}Rb during the initial portion of the washout curve. The mean early FER for ^{83}Rb (0.0060 ± 0.0026 s^{-1}), exceeded that for ^{201}Tl (0.0018 ± 0.0008 s^{-1}) ($P < 0.0001$) (Fig. 7). The early FER values increased with flow ($P < 0.0001$ for ^{201}Tl and ^{83}Rb). The slopes were 0.0009 ml^{-1} min g and 0.0029 ml^{-1} min g for ^{201}Tl and ^{83}Rb, respectively. To assess late FER, we analyzed the average FER over the last 10 data points of the indicator dilution curve. The mean late FER for ^{83}Rb (0.00020 ± 0.00015 s^{-1}) was less than that of ^{201}Tl (0.00035 ± 0.00022 s^{-1}) ($P < 0.0001$). Flow had no effect on late FER (^{201}Tl, $P < 0.34$; ^{83}Rb, $P < 0.82$).

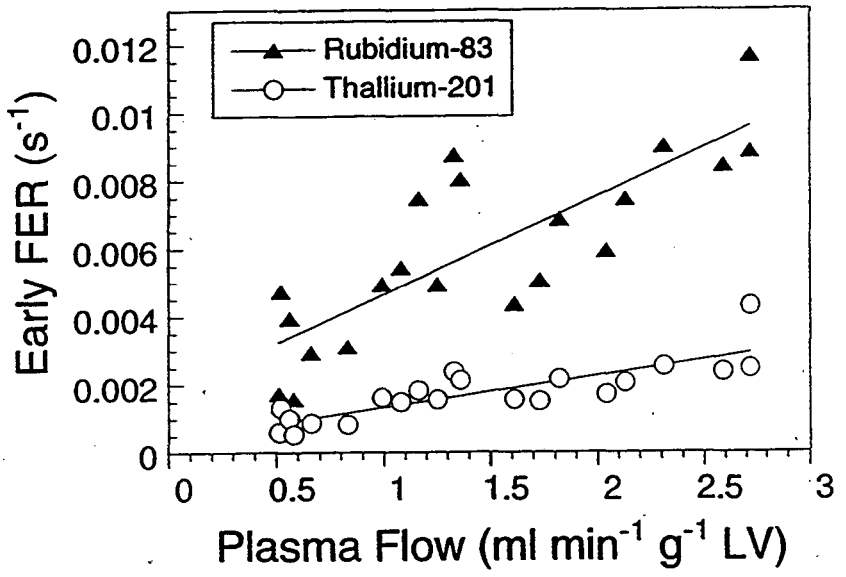

Figure 7. The early fractional escape rates as a function of plasma flow. The lines through the data points were determined by linear regression. The *R* values were 0.73 for ^{201}Tl and 0.74 for ^{83}Rb.

^{201}Tl and ^{83}Rb Net Uptake. We define the net tracer uptake, *U(t)*, to be the product of flow and net tracer retention. The maximum values of *U*, U_{max}, for ^{201}Tl and ^{83}Rb are shown as a function of flow in Fig. 8*A* and 8*B*, respectively. *U(t)* at $t = 2$ min are shown in Fig. 8*C* and 8*D*. The dashed line of identity would result if net tracer retention were 100%. U_{max} for ^{83}Rb was somewhat closer to the line of identity than U_{max} for ^{201}Tl. However, by 2 min ^{201}Tl uptake was closer to the line of identity than ^{83}Rb uptake.

^{201}Tl and ^{83}Rb Net Retention. Tracer retention as measured by $E_{net}(t)$ reflects both initial tracer extraction and subsequent tracer washout. As predicted by the higher initial extraction of ^{83}Rb versus ^{201}Tl, ^{83}Rb mean maximum E_{net} (0.75 ± 0.12) is greater than ^{201}Tl mean maximum E_{net} (0.65 ± 0.09) ($P < 0.0001$). In contrast, the mean E_{net} at 2 min for ^{83}Rb (0.32 ± 0.09) was significantly less than E_{net} at 2 min for ^{201}Tl (0.55 ± 0.08) ($P < 0.0001$). The greater early washout of ^{83}Rb compared to ^{201}Tl is presumably responsible for the rapid reduction in ^{83}Rb retention compared to ^{201}Tl. Although calculated differently, the reduced retention of ^{83}Rb versus ^{201}Tl at 2 min is directionally similar to that observed with deconvolution analysis, where the late retention of ^{83}Rb was significantly less than ^{201}Tl as estimated by fitting a single decaying exponential to the tail of the impulse response function.

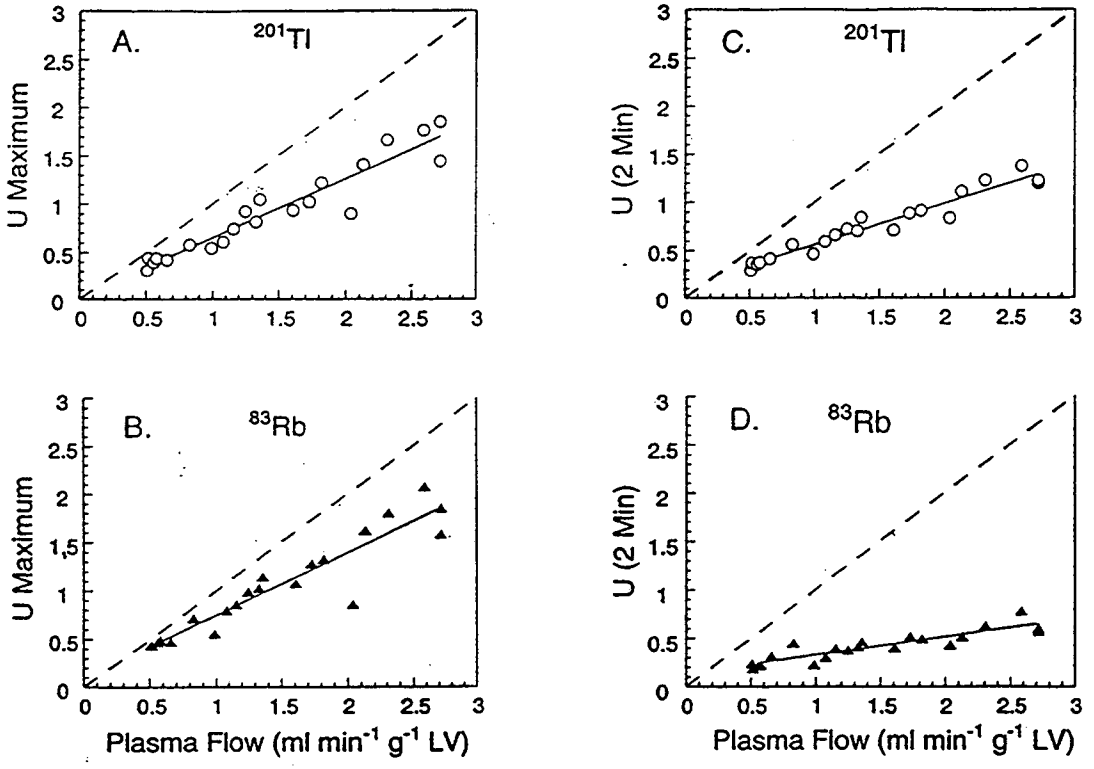

Figure 8. The relationship between ^{201}Tl and ^{83}Rb uptake and flow. The Y-axis represents an $E_{net}(t)$ value multiplied by the corresponding plasma flow (F) for each experiment. The equations for the linear fits to the data points (solid line) and the R values are as follows. Panel A, F x E_{net} maximum for ^{201}Tl; $y = 0.030 + 0.615x$, $R = 0.955$. Panel B, F x E_{net} maximum for ^{83}Rb; $y = 0.112 + 0.642x$, $R = 0.931$. Panel C, F x E_{net} at 2 min for ^{201}Tl; $y = 0.148 + 0.419x$, $R = 0.967$. Panel D, F x E_{net} at 2 min for ^{83}Rb; $y = 0.139 + 0.193x$, $R = 0.885$. The dashed lines are lines of identity.

Volume of Distribution for ^{201}Tl and ^{83}Rb

The observation that thallium is better retained in the myocardium suggests that thallium might have greater access to the intracellular potassium pool. In six experiments, the V_d for ^{201}Tl (13.4 ± 3.5) exceeded that for ^{83}Rb (11.0 ± 2.5) ($P < 0.05$) (Fig. 9).

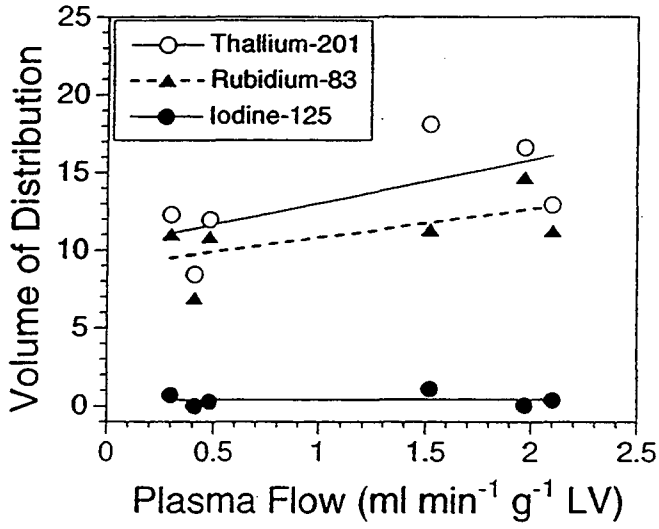

Figure 9. The mean volume of distribution (V_d) for ^{201}Tl, ^{83}Rb, and ^{125}I-albumin. The lines through the data points were determined by linear regression.

Discussion

In this investigation, the multiple indicator dilution technique was used to assess the extraction, retention, and washout of ^{201}Tl and ^{83}Rb in the presence of an intravascular tracer, ^{125}I-albumin. Two distinct computational approaches were used. The first approach was designed to separate the effects of circulatory tracer dispersion, as measured by the ^{125}I-albumin reference curve, from extravascular movement of flow tracer. The fundamental concept behind this approach is that the diffusible tracer curves can be modeled as the convolution of the ^{125}I-albumin curve, which reflects circulatory dispersion, and the impulse-response function of the myocardium, which reflects the extravascular movement of ^{201}Tl and ^{83}Rb. The computed impulse response provided a description of the myocardial extraction and retention of ^{201}Tl and ^{83}Rb that was independent of circulatory dispersion.

In the second approach, which we term the conventional approach, we computed a number of indices for extraction and retention that have been commonly used in the literature. These indices were initially proposed by investigators interested in estimating the uni-directional flux of solutes

out of the capillary into the extravascular space. Attention was focused on the initial portion of the venous curves (to minimize the effects of back-diffusion of tracer from the extravascular space) with the difference between the early vascular reference curve and the early venous tracer curve used to compute a fractional extraction. No direct attempts were made to separate the effects of circulatory tracer dispersion from extravascular movement of tracer. Together with fractional escape rate to evaluate tracer washout, these indices have been used successfully to estimate capillary solute exchange in addition to evaluating flow tracer uptake and retention by a number of investigators (2, 6, 10, 15, 17-19, 21).

Both methods of analysis demonstrated some striking differences in the kinetic behavior of ^{201}Tl and ^{83}Rb. The initial extraction of ^{83}Rb was observed to be slightly higher than that of ^{201}Tl. This is likely due, in part, to the preferential uptake of thallium into red blood cells. A more impressive difference is in the rapid washout of tracer. There was considerably more washout of ^{83}Rb than ^{201}Tl immediately after the introduction of the tracer (roughly in the 10–120 s time period). Another major difference is in the net retention of ^{201}Tl and ^{83}Rb. Using the conventional analysis and E_{net} at 2 min, net retention of ^{201}Tl was considerably greater than ^{83}Rb. Similarly, fractional retention of ^{201}Tl was approximately double that for ^{83}Rb from 10–30 min after tracer injection using the deconvolution analysis. Taken together, these results indicate that ^{83}Rb and ^{201}Tl are handled quite differently by the myocardium, with ^{201}Tl appearing to be better retained than ^{83}Rb over most of the time period investigated in this study. These data suggest that, in this simple non-recirculating experimental model, thallium tissue content provides a better indicator of regional flow than rubidium within a few minutes of tracer introduction.

Although results from the deconvolution and conventional analyses were in basic agreement, the two approaches disagreed on the effect of flow on both early and late tracer washout. Early tracer washout, as estimated by FER*(t)* in the conventional method, was positively correlated with plasma flow rate for both ^{201}Tl and ^{83}Rb. In contrast, early ^{83}Rb washout, as judged by the time integral of the impulse response curves from 5 to 30 s, was unaffected by flow. A probable explanation for this disagreement is that FER*(t)* includes tracer washout from the intravascular space, while the time integral of the impulse response function explicitly evaluates washout of tracer from the extravascular space only. Since intravascular tracer dispersion is inversely related to flow, it seems likely that early FER values are affected by this inverse relationship, while the impulse response function is not. Late tracer washout, as assessed by the rate constants of the exponential function fitted to the tail of the impulse response obtained in the deconvolution analysis, was positively correlated with the flow, while late tracer washout evaluated by late FER values was unaffected by flow. The most likely explanation for this discrepancy is that there was considerable scatter in late FER values secondary to low values in the residue function (see *Eq. 6* and *7*). The scatter in the

late FER values appears to diminish the accuracy with which late tracer washout is estimated by this computation and could account for this disagreement.

There are some important differences between the conventional and deconvolution analysis approaches used in this study. The conventional quantity $E(t)$ is a true measure of uni-directional tracer extraction only if back-diffusion is zero (15). Our results indicate that, particularly for rubidium, there is a significant amount of back-diffusion in the system under study. Thus $E(t)$ gives only an approximation to true tracer extraction. In contrast, the deconvolution analysis approach can completely compensate for back-diffusion, limited only by the temporal resolution of venous sampling rate. Moreover, the conventional indices are, to a greater or lesser extent, all affected by circulatory dispersion. Therefore use of these indices to study tracer extraction and retention as a function of flow is confounded by the inverse relationship between flow and circulatory dispersion (that is, at high flow the tracer bolus is less temporally dispersed). Since the deconvolution analysis approach explicitly removes the effects of circulatory dispersion, it provides a more refined tool for assessing the effects of flow on tracer extraction and retention.

This study provides some clues about capillary conductance and bi-directional cell membrane transport for thallium and rubidium. E_{peak} is often interpreted as providing a measure of the uni-directional flux across the capillary wall (10, 11, 18). Our E_{peak} values for ^{83}Rb were similar to published values for thallium (and potassium) suggesting that the uni-directional flux (or conductance) across the capillary wall is similar for these substances (3, 18, 25). However, our extraction indices for ^{201}Tl were lower than previously reported values. This latter observation might be an artifact due to red blood cell uptake.

In the present study, the net retention of thallium was considerably greater than that of rubidium over most of the 20–30 min experiment time periods evaluated here, while the rate of washout of extracted rubidium was significantly greater than that of thallium starting approximately 20 s after isotope introduction. One interpretation of these observations is that thallium preferentially crosses the sarcolemma into the myocyte and is thus unavailable for back-diffusion from the interstitial space into the vascular compartment (J. B. Bassingthwaighte, personal communication). In contrast, rubidium does not enter the myocyte as rapidly as thallium, is retained in the interstitial space, and is therefore available for back-diffusion into the vascular space with subsequent washout from the heart. Assuming the slow component, assessed from the tail of the impulse response function, represents tracer inside the myocyte, the information obtained with our deconvolution analysis supports this proposed mechanism in which thallium has greater access to the intracellular potassium pool than rubidium. Similarly, the conventional analysis showed that net retention of ^{201}Tl is greater than ^{83}Rb as early as 2 min after tracer introduction. This hypothesis is also supported by the observation that the V_d for thallium was greater than for rubidium. Since there is no reason to suppose that the intravascular and the interstitial volumes of distribution are different

for these two flow tracers, these results suggest the myocyte accumulates more thallium than rubidium.

In recent work using a more detailed mechanistic model (J. B. Bassingthwaighte, personal communication) the permeability surface area product of the sarcolemma for thallium was found to be 2–3 times higher than that for potassium. One potential explanation provided by these investigators is that thallium might be transported into the myocyte via sodium channels in addition to potassium channels and possibly by the sodium-potassium ATPase pump. This observation strongly suggests that myocyte transport of ^{201}Tl is quantitatively different and more efficient than that of potassium (and probably rubidium).

Although there are obvious differences between the current data and data obtained in *in vivo* studies, the results reported here could have relevance to clinical studies. One major difference is that, in contrast to the constant flow, steady-state experimental design employed here, most clinical studies are performed during stress/rest, non-steady-state conditions. Second, in the present study, kinetic data for ^{201}Tl and ^{83}Rb were obtained following delivery of a compact tracer bolus directly to the myocardium. In contrast, substantial tracer dispersion following intravenous isotope injection and tracer recirculation is inevitable in human studies. Conceptually, the signal obtained from human hearts can be viewed as representing the summation of myocardial extraction, retention, and washout for multiple, very small sequential tracer boluses. Provided the data obtained in rabbit hearts are applicable to humans, the extraction, retention, and washout kinetics of each of these individual boluses would be similar to that observed here in the individual rabbit hearts following bolus introduction of the tracer. Relative to the present data, the net effect of prolonged tracer delivery to the myocardium in clinical studies is to lengthen the period of net myocardial ^{201}Tl and ^{83}Rb uptake and retention, and delay net washout.

In summary, the relationship between ^{201}Tl and ^{83}Rb tissue tracer content and flow has been evaluated in the isolated RBC/albumin perfused rabbit heart using the multiple indicator dilution technique and two distinct computational approaches. The first approach explicitly deconvolved the thallium and rubidium venous concentration curves by the vascular reference tracer curve to separate the effects of circulatory dispersion from myocardial extraction and retention of thallium and rubidium. The second approach used a conventional analysis to compute thallium and rubidium extraction, retention, and washout. Both approaches showed that there was substantial early washout of initially extracted ^{83}Rb and that ^{201}Tl was better retained by the myocardium for most of the 20–30 min experimental time periods evaluated here. Since clinical evaluation of myocardial perfusion uses the generator produced, short-lived (76 s physical half-life) positron-emitting isotope ^{82}Rb (4), the relatively rapid washout of ^{83}Rb (86 d half-life) might not adversely affect the use of ^{82}Rb.

Acknowledgements

The authors wish to thank Ms. Heidi Maurer and Ms. Lisa R. Williams for their valuable technical assistance. This work was supported in part by the Director, Office of Energy Research, Office of Health and Environmental Research, Medical Applications and Biophysical Research Division of the U. S. Department of Energy under contract No. DE-AC0376SF00098 and in part by the National Institute of Health, National Heart, Lung and Blood Institute under grants Nos. HL25840 and HL48068.

References

1. Bassingthwaighte, J.B. and C.A. Goresky. Modeling in the analysis of solute and water exchange in the microvasculature. In: *Handbook of Physiology: Microcirculation*, edited by E.M. Renkin and C.C. Michel. Bethesda, Maryland: American Physiological Society, 1984, vol. IV, part 1, p. 549–626.

2. Bassingthwaighte, J.B., G.M. Raymond and J.I. Chan. Principles of tracer kinetics. In: *Nuclear Cardiology: State of the Art and Future Directions*, edited by B.L. Zaret and G.A. Beller. St. Louis, MO: Mosby-Year Book, Inc., 1993, p. 3–23.

3. Bergmann, S.R., S.N. Hack and B.E. Sobel. "Redistribution" of myocardial thallium-201 without reperfusion: Implications regarding absolute quantification of perfusion. *Am. J. Cardiol.* 49: 1691–1698, 1982.

4. Budinger, T.F., Y. Yano and B. Hoop. A comparison of $^{82}Rb^{+}$ and $^{13}NH_3$ for myocardial positron scintigraphy. *J. Nucl. Med.* 16: 429–31, 1975.

5. Chinnard, F.P., G.J. Vosburgh and T. Enns. Transcapillary exchange of water and of other substances in certain organs of the dog. *Am. J. Physiol.* 183: 221–234, 1955.

6. Crone, C. Permeability of capillaries in various organs as determined by the indicator diffusion method. *Acta Physiol. Scand.* 58: 292–305, 1963.

7. Gamel, J., W.F. Rousseau, C.R. Katholi and E. Mesel. Pitfalls in digital computation of the impulse response of vascular beds from indicator-dilution curves. *Circ. Res.* 32: 516–523, 1973.

8. Goldhaber, S.Z., J.B. Newell, J.S. Ingwall, G.M. Pohost, N.M. Alpert and E.T. Fossell. Effects of reduced coronary flow on thallium-201 accumulation and release in an in vitro rat heart preparation. *Am. J. Cardiol.* 51: 891–896, 1983.

9. Grunwald, A.M., D.D. Watson, H.H. Holzgrefe, Jr., J.F. Irving and G.A. Beller. Myocardial thallium-201 kinetics in normal and ischemic myocardium. *Circ.* 64: 610–618, 1981.

10. Guller, B., T. Yipintsoi, A.L. Orvis and J.B. Bassingthwaighte. Myocardial sodium extraction at varied coronary flows in the dog: estimation of capillary permeability by residue and outflow detection. *Circ.* 37: 359–378, 1975.

11. Huang, S.C., B.A. Williams, J. Krivokapich, L. Araujo, M.E. Phelps and H.R. Shelbert. Rabbit myocardial ^{82}Rb kinetics and a compartmental model for blood flow estimation. *Am. J. Physiol.* 256: H1156–H1164, 1989.

12. Krivokapich, J. and K.I. Shine. Effects of hyperkalemia and glycoside on thallium exchange in rabbit ventricle. *Am. J. Physiol.* 240: H612–H619, 1981.

13. Krivokapich, J., C.R. Watanabe and K.I. Shine. Effects of anoxia and ischemia on thallium exchange in rabbit myocardium. *Am. J. Physiol.* 249: H620–H628, 1985.

14. Kuruc, A., W.J. Caldicott and S. Treves. An improved deconvolution technique for the calculation of renal retention functions. *Comp. Biomed. Res.* 15: 46–56, 1982.

15. Lassen, N.A. and C. Crone. Extraction fraction of a capillary bed to hydrophobic molecules: Theoretical considerations regarding the singes injection technique with a discussion of the role of diffusion between laminar streams. In: *Capillary Permeability*, edited by C. Crone and N.A. Lassen. Copenhagan: Munksgaard, 1970, p. 48–59.

16. Lawson, C.L. and R.J. Hanson. *Solving Least Squares Problems*. Englewood Cliffs, NJ: Prentice-Hall, Inc., 1974.

17. Leppo, J.A. Myocardial uptake of thallium and rubidium during alterations in perfusion and oxygenation in isolated rabbit hearts. *J. Nucl. Med.* 28: 878–885, 1987.

18. Leppo, J.A. and D.J. Meerdink. Comparison of the myocardial uptake of a technetium-labeled isonitrile analogue and thallium. *Circ. Res.* 65: 632–639, 1989.

19. Little, S.E., J.M. Link, K.A. Krohn and J.B. Bassingthwaighte. Myocardial extraction and retention of 2-iododesmethylimipramine: a novel flow marker. *Am. J. Physiol.* 250: H1060–H1070, 1986.

20. Marshall, R.C. Correlation of Contractile Dysfunction with Oxidative Energy Production and Tissue High Energy Phosphate Stores during Partial Coronary Flow Disruption in Rabbit Heart. *J. Clin. Invest.* 82: 86–95, 1988.

21. Marshall, R.C., E.M. Leidholdt, Jr., D.Y. Zhang and C.A. Barnett. Technetium-99m hexakis 2-methoxy-2-isobutyl isonitrile and thallium-201 extraction, washout, and retention at varying coronary flow rates in rabbit heart. *Circ.* 82: 998–1007, 1990.

22. Marshall, R.C., W.W. Nash, M.M. Bersohn and G.A. Wong. Myocardial energy production and consumption remain balanced during positive inotropic stimulation when coronary flow is restricted to basal rates in rabbit heart. *J. Clin. Invest.* 80: 1165–1171, 1987.

23. Mullani, N.A., R.A. Goldstein, K.L. Gould, S.K. Marani, D.J. Fisher, H.A. O'Brien, Jr. and M.D. Loberg. Myocardial perfusion with rubidium-82. I. Measurement of extraction fraction and flow with external detectors. *J. Nucl. Med.* 24: 898–906, 1983.

24. Sheehan, R.M. and E.M. Renkin. Capillary, interstitial, and cell membrane to blood-tissue transport of potassium and rubidium in mammalian skeletal muscle. *Circ. Res.* 30: 588–607, 1972.

25. Weich, H.F., H.W. Strauss and B. Pitt. The extraction of thallium-201 by the myocardium. *Circ.* 56: 188–191, 1977.

LAWRENCE BERKELEY LABORATORY
UNIVERSITY OF CALIFORNIA
TECHNICAL INFORMATION DEPARTMENT
BERKELEY, CALIFORNIA 94720